CHARACTERIZING THE INTERNAL MORPHOLOGY OF TRANSITION REGIONS IN LARGE-SCALE EXTRUSION DEPOSITION ADDITIVE MANUFACTURING

James Brackett[1], Zaky Hussein[2], Elijah Charles[2], Tyler Smith[3], Ahmed Hassen[3], Seokpum Kim[3], Vlastimil Kunc[3], Chad Duty[2,3]

[1] The Bredesen Center for Interdisciplinary Research and Graduate Education, University of Tennessee – Knoxville, TN
[2] Mechanical, Aerospace, and Biomedical Engineering, University of Tennessee – Knoxville, TN
[3] Oak Ridge National Laboratory, Oak Ridge, TN

Abstract

A dual-hopper feed system that was developed for the Big Area Additive Manufacturing (BAAM) system allows for transitioning between different materials while maintaining continuous deposition. This technique creates a step-change in material feedstock by switching the pellet feeding system to alternate which hopper is currently supplying material, allowing for multi-material construction. The step-change in feedstock material produces a transition region that is characterized by a compositional gradient and blended internal morphology. Initial cross-sectional imaging of the transition region revealed a non-homogenous blend of materials with distinct domains of each material, likely due to incomplete mixing within the screw. This study used a carbon fiber reinforced acrylonitrile butadiene styrene (CF-ABS) and an unfilled ABS to characterize the internal structure and to correlate it to mechanical performance by tracking microhardness across cross-sections of the transition region.

Introduction

Large-Format Additive Manufacturing (LFAM) has seen a rapid increase in interest in recent years, evidenced by the increasing number of systems available. Some examples include Cincinatti Incorporated's Big Area Additive Manufacturing (BAAM) system featured in recent literature [1-3], Thermwood's commercially available Large Scale Additive Manufacturing (LSAM) system [4-6], and even international efforts such as this custom prototype Polymeric Pellet-Based Additive Manufacturing (PPBAM) system [7].

One of the more prevalent research areas is the introduction of multi-material capabilities. For example, recent developments with the BAAM have seen the introduction of a dual-hopper system capable of automated, on-the-fly material switching [2]. The system complements the pelletized feedstock by introducing a step-change in material feedstock then allowing the extrusion screw to blend pellets of differing composition and produce a continuous transition from Material A to Material B. Figure 1 shows an example schematic of the process, indicating key transition points (1A, 1B, 1C). After purging Material A through the system to reach steady-state, the hopper switch would be initiated at 1A. From there, there is remaining Material A still in the extrusion barrel that must exit before the blended region begins at 1B. The transition continues until 1C where a steady-state Material B has been reached. This is also shown graphically with the y-axis indicating material composition and x-axis representing volume of extruded material.

Figure 1: A schematic representation of a printed material transition using the BAAM Dual-Hopper system where blue represents Material A and red represents Material B.

This approach avoids some of the typical pitfalls of multi-material extrusion with thermoplastics by eliminating discrete material boundaries and the need to stop the extrusion process to switch materials. However, the blended transition region presents other possible issues. As shown in Figure 2, cross-section images taken from the transition region where material blending occurs shows distinct regions of both Material A (acrylonitrile butadiene styrene, ABS) and Material B (20 wt % carbon-fiber filled ABS, CF-ABS). The heterogeneous internal morphology could have distinct effects on the mechanical performance of the transition region.

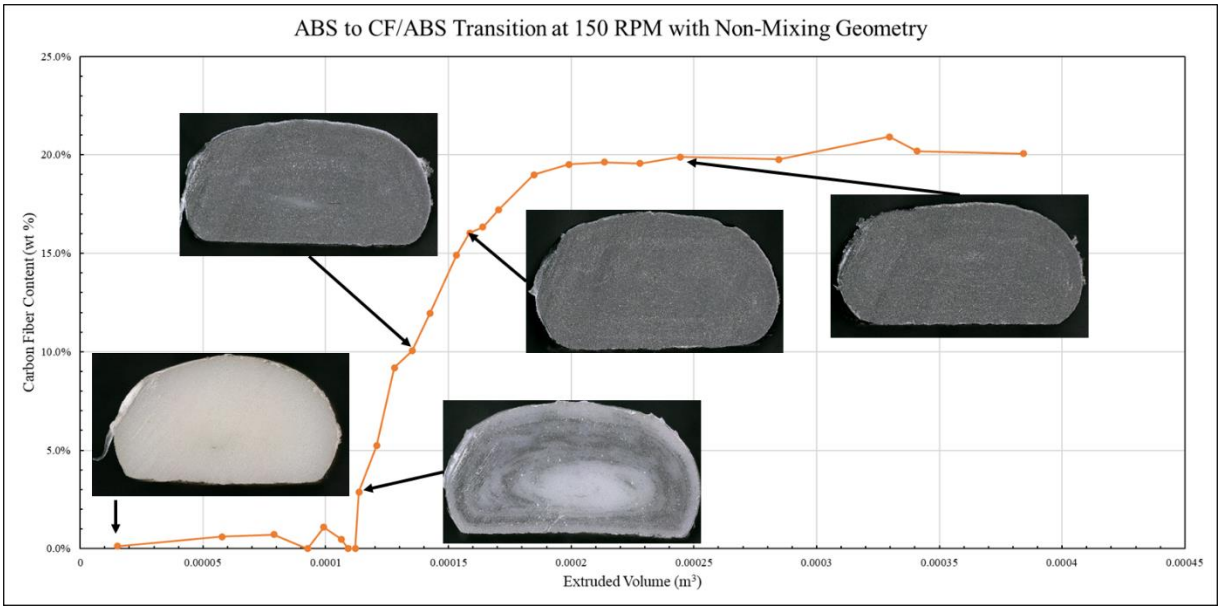

Figure 2: The change in fiber content of a printed material transition from neat ABS to CF/ABS as a function of extruded volume. Images are cross-sections that were taken from the indicated point in the transition.

Investigating the mechanical behavior of a single printed bead can be difficult, especially when trying to discern differences between regions in the cross-section. As such, hardness measurements provide a unique opportunity to investigate deformation resistance on a local scale using microhardness indentation. Typically, thermoplastics are submitted to Shore hardness testing using a durometer [8], as was done by Vian and Denton in this study comparing the change in hardness with processing conditions [9]. For other studies, particularly those focused on microhardness, a Vickers Hardness system was used. Zheng and Ashcroft used microhardness indentation to investigate the effectiveness of various adhesives and their application to a part [10]. Turnbull and White utilized microhardness in an in-depth characterization study of unplasticized poly-vinyl chloride [11]. Another similar study saw a change in Vickers hardness with differences

in nanoparticle fillers using microhardness testing at a variety of applied loads [12]. A comprehensive study of a dental composite material evaluated its resistance to deformation and established an increased stability in results with higher loads and longer dwell times [13].

Characterizing the mechanical behavior of the transition region created when switching materials with the dual-hopper BAAM system is critical to understanding how the blended material composition will affect overall part performance. The first step in this process is understanding how the internal morphology changes with processing conditions and the effect of the regional morphology. Vickers microhardness indentation provides a tool well-suited for characterizing the limited area provided by a single-bead cross-section. This study will utilize hardness measurements to represent local resistance to deformation and examine differences in performance based on regional composition. The effect of changes in processing conditions will also be investigated.

Experimental Methods

All samples were printed using the BAAM dual-hopper system. Three sample sets were created to isolate the effects of bot extrusion screw geometry and direction of material transition. Samples were extracted from locations of interest in each of the three transitions. Carbon fiber content was measured via Ultrasonic-Assisted Acid Digestion, as described in previous work [3, 14]. Vickers microhardness was measured at multiple locations on each cross-sectional sample.

Print Conditions

Print conditions and materials were constant for all printed samples. Techmer Engineered Solutions provided both a neat ABS resin (HIFILL ABS 1512 3DP) and a 20 wt % CF/ABS (ELECTRAFIL ABS 1501 3DP) for sample production. Material feedstock was dried at 80 °C for at least four hours. Thermal processing conditions were kept constant regardless of which hopper was in use, maintaining a bed temperature of 100 °C and melt temperature of 250 °C. Using a 10 mm (0.4 in) diameter nozzle, each structure was printed with bead dimensions of 5 mm (0.2 in) by 14 mm (0.55 in).

Sample Preparation

All material transitions were printed as a single continuous bead using a dual-hopper equipped BAAM at ORNL's Manufacturing Demonstration Facility. Three different parameter sets that varied either screw geometry or transition direction were used in this study: Non-mixing ABS to CF/ABS, Mixing ABS to CF/ABS, and Non-Mixing CF/ABS to ABS. All other system parameters were held constant. Cross-sectional samples 10 mm long were extracted using an Isomet 1000 Precision saw from five locations within each printed transition. The five cross-sections were chosen based on visual appearance and measured fiber content. One was taken from both the neat ABS and CF/ABS regions while three samples were taken from the transition regions. The specimens from the transition region were confirmed to be of similar fiber content to those taken from the other transitions by previous work [15].

Each of the fifteen cross-sections were embedded in an EpoxiCure 2 epoxy disc and polished with the same procedure. A six-slot AutoMet 250 autopolisher was used to grind the reverse side of the discs flat using 240, 320, 400, 600 and 800 SiC grit paper in sequence. The cross-sectional surface was polished with 240, 320, 400, 600, 800, and 1200 SiC grit for 1 minute each with 2 lb central force. The sample holder was set to 60 RPM at a contrary rotation to the polishing platen (120 RPM). The surface was finished using a 6 μm diamond suspension with complimentary rotation of the sample holder for 5 minutes.

Microhardness Measurements

Microhardness indentation was conducted using a Wilson VH1202 Micro Hardness Tester following ASTM E384 [16]. Based on literature [11, 13], a 100 gf load and 15 s dwell time was used for all indentations to reduce variance as much as possible. Vickers Hardness (HV) values were calculated by the instrument using the measured diagonals. The indentation pattern for each cross-section was a rough cross shape, as seen in Figure 3, with a 1 mm spacing. Each indent is circled in green. This pattern provided an unbiased selection of data points to analyze possible variance in the heterogenous morphology. The average HV and standard deviation were recorded for each cross-sectional sample. Any indentations hindered by porosity or sample defects were not considered. Average HV and standard deviations were plotted as a function of fiber content.

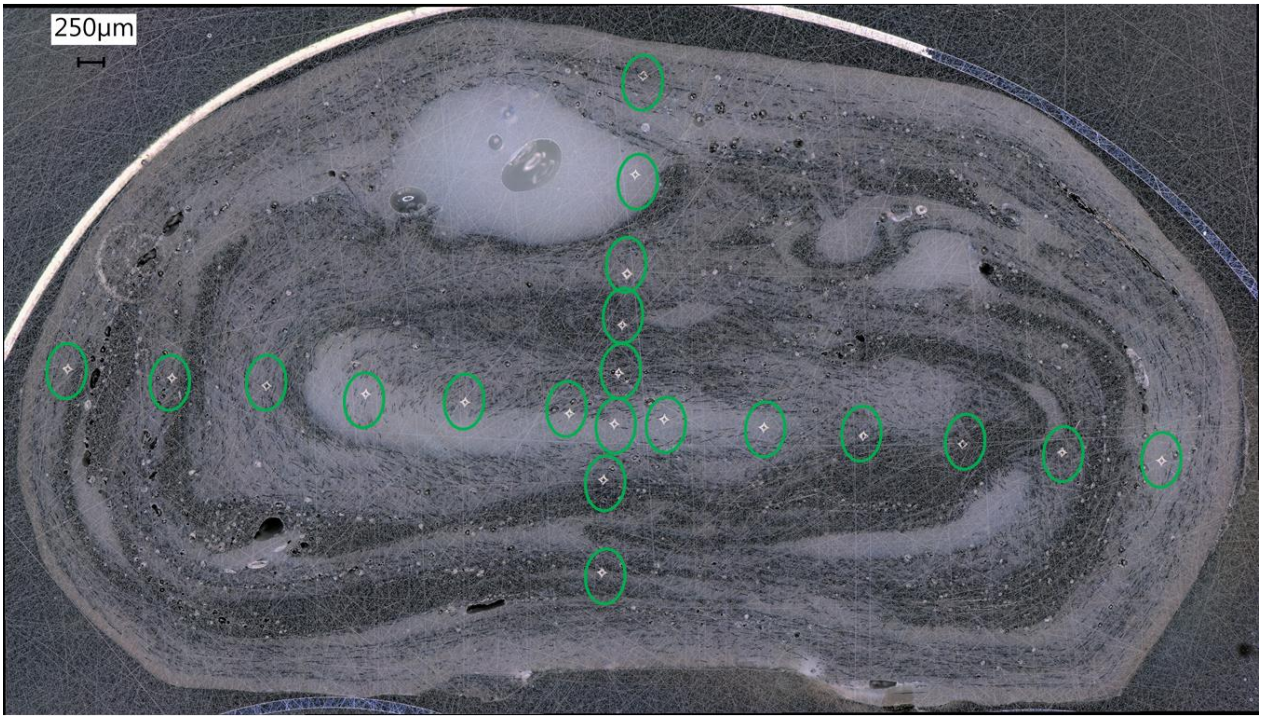

Figure 3: An example of the pattern used when making microhardness indentations on the studied cross-sections. The indents are circled in green.

Optical Microscopy

Each cross-section was imaged with a Keyence VHX-5000 digital microscope. To capture a detailed image of the entire cross-section, the 2D-stitching software was used at 200x magnification. These images were used to assess whether an indentation had been hindered by sample defects. Furthermore, the images were used to identify three distinct regions (neat ABS, mixed, and carbon-fiber rich) present in the cross-sections and determine in which region each indentation fell. Figure 4 provides an example of how each region was differentiated; blue, purple, and red represent the neat ABS, mixed, and fiber-rich regions, respectively.

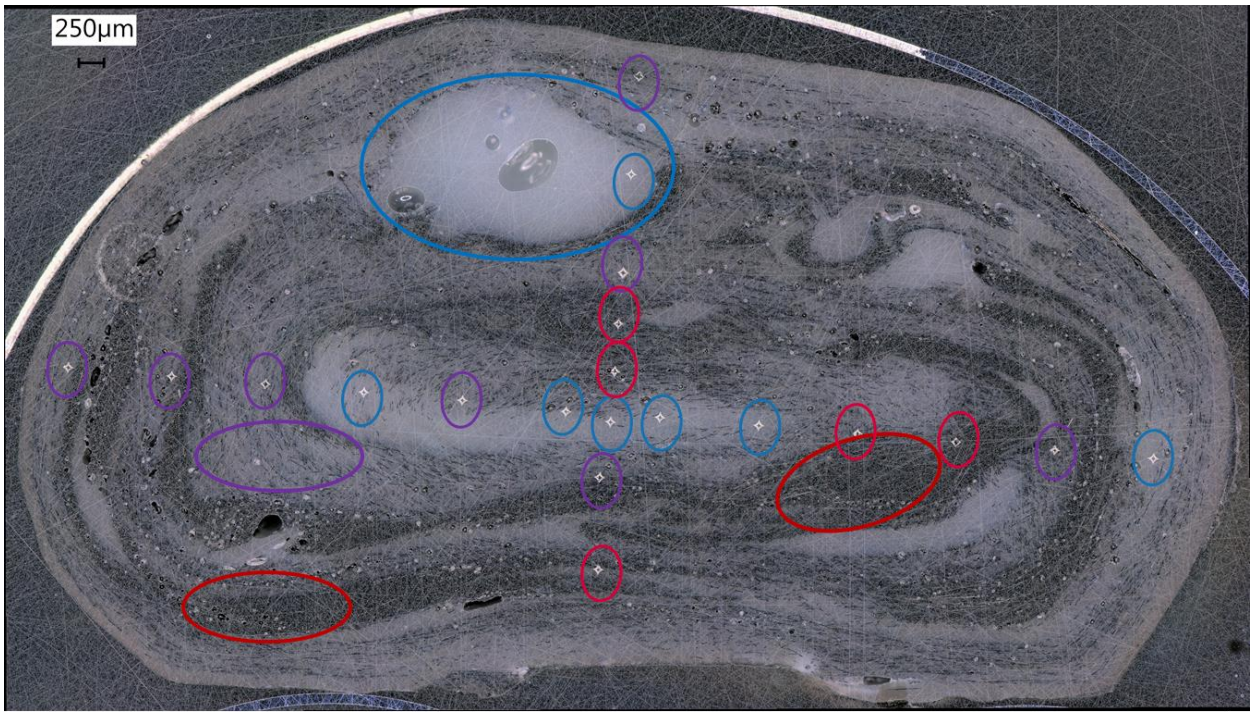

Figure 4: An example of the different regions observed in sample imaging. Color-coding indicates the region an indent fell in.

Results and Discussion

Regional Variance of Microhardness

The measured HV of each indentation on a representative cross-section were compared to analyze the change in HV compared to change in surrounding material composition. Using the same sample from Figures 3 and 4, Figure 5 shows the HV of two indentations from each of the three regions. Once again, the blue, purple, and red signified neat ABS, mixed, and fiber-rich regions respectively. The results indicated a clear increase in HV with increasing fiber content in the surrounding areas. This trend was consistent across all cross-sections, with fiber-rich regions displaying an increased resistance to indentations, resulting in a higher measured HV.

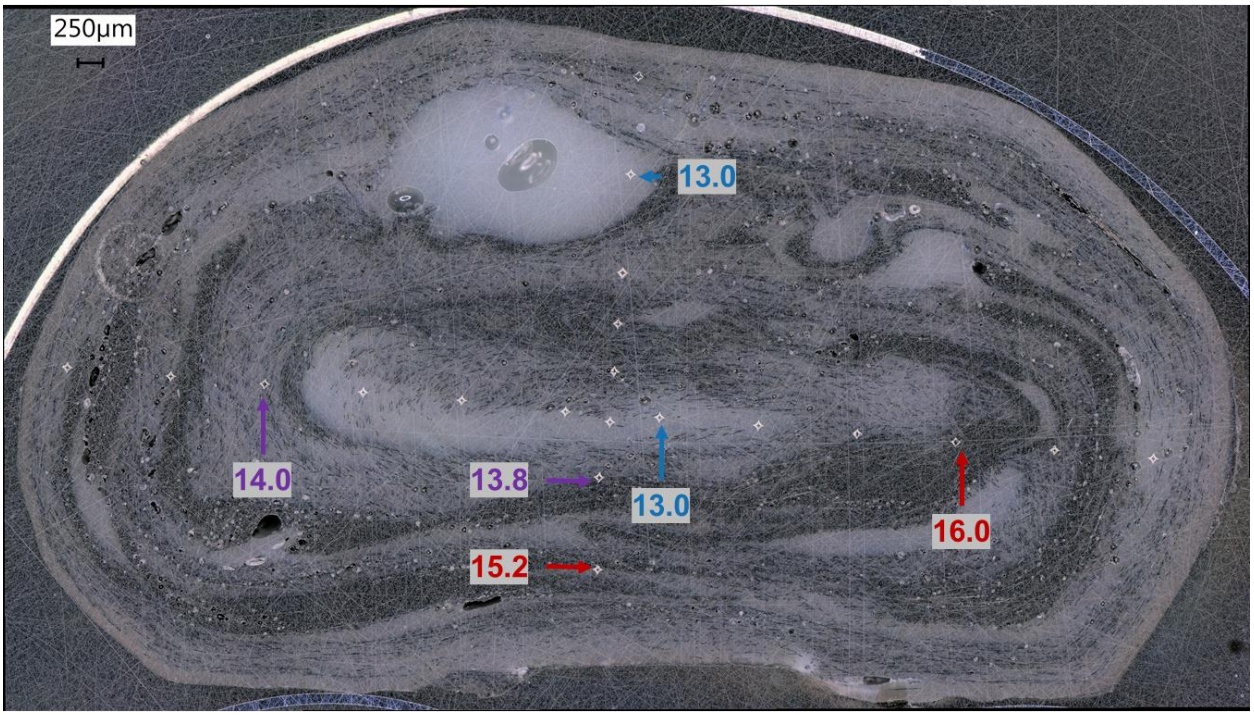

Figure 5: The hardness values of several indents demonstrating the change in hardness based on region.

Following confirmation of variance with fiber content, the fiber content of the horizontal line of indents was plotted as a function of distance from the left edge. As shown in Figure 6 there was minimal correlation between horizontal positioning on the cross-section. Furthermore, the increase of overall fiber content did not eliminate instances of low hardness values. This remained true when considering the vertical selection of indents.

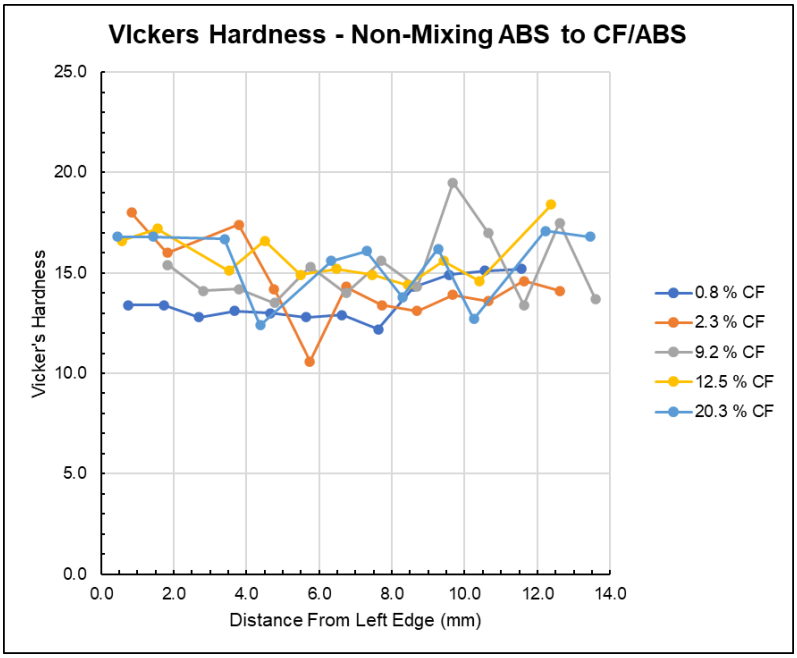

Figure 6: Vickers Hardness values of the horizontal indents for five samples of differing fiber content taken from the same printed transition.

Average Vickers Hardness

While there was not an apparent trend in the measured HV in relation to location on the cross-sectional surface, there was an obvious trend for the average HV across all samples in each set. Beginning with the Non-mixing, ABS to CF/ABS sample set, Figure 7 shows the Average Vickers Hardness value and standard deviation of the indentations on each cross-section as a function of fiber content. As fiber content increases, the average hardness steadily rises from 13.2 HV to 16.4 HV, an increase of 24 %. Similarly, the standard deviation increases with increasing fiber content, rising by 300 % from 0.27 to 1.08. This indicates that, as expected, the increased presence of the fibers results in an increased resistance to deformation. Furthermore, the increased variation at higher fiber contents suggests that the poor mixing allows for regions of significantly different mechanical characteristics.

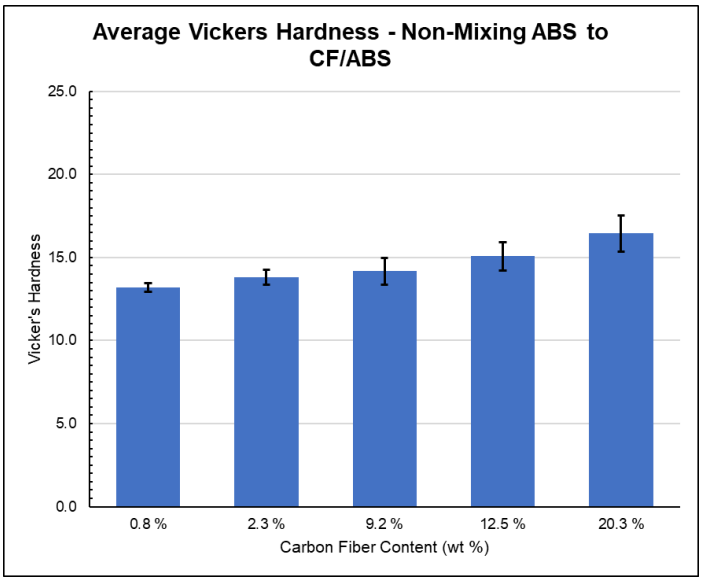

Figure 7: The average Vickers hardness value and standard deviation of all viable indents for each sample.

Figures 8a and 8b show similar trends for the other two sample sets: an ABS to CF/ABS transition printed using a screw geometry intended to improve mixing (Mixing ABS to CF/ABS) and a CF/ABS to ABS transition printed using the same non-mixing screw geometry as the first sample set (Non-Mixing CF/ABS to ABS). As seen in 6a, the average hardness and standard deviation still increase with fiber content (about 36 % and 270%, respectively) despite the change in screw geometry. While the maximum of 17.6 HV is a 7 % increase compared to the Non-mixing screw geometry, the maximum standard deviation also showed a small increase from 1.08 to 1.10. This indicates that the mixing geometry provided minimal improvements in mixing and producing a more homogenous internal morphology. Once again, the Non-Mixing CF/ABS to ABS transition shown in Figure 8b showed an increasing hardness value and standard deviation with increasing fiber content. A maximum 19.0 HV represented an 8 % and 15 % increase compared to the Mixing and Non-Mixing ABS to CF/ABS transitions, respectively. Similarly, the maximum standard deviation increased by 61 %. Within the CF/ABS sample set, average HV increased by 45 % whereas the standard deviation increased by 620 %.

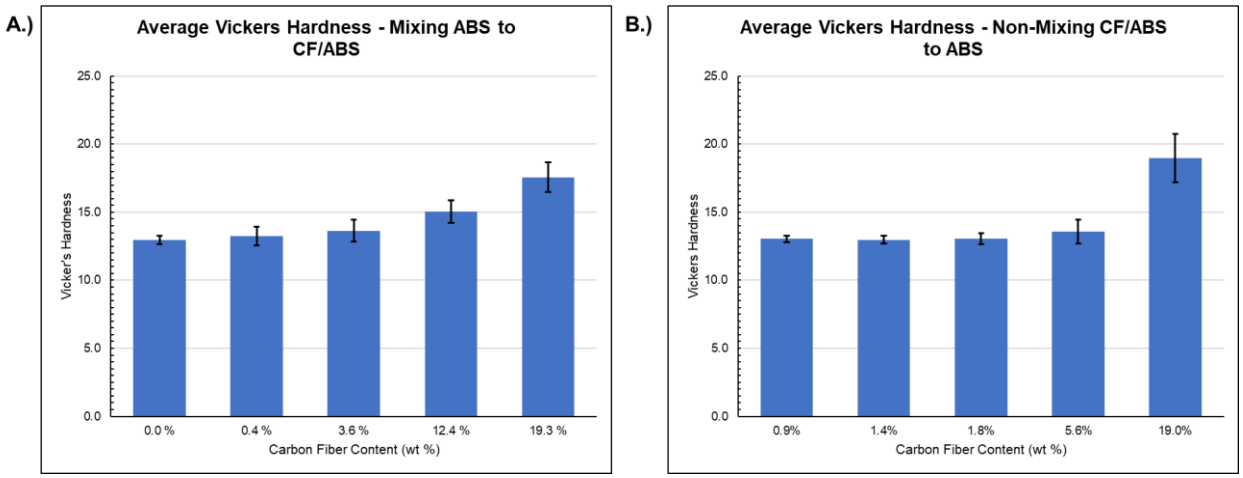

Figure 8: A.) the average Vickers hardness for each cross-section from the Mixing ABS to CF/ABS sample set, and B.) the average Vickers hardness for each cross-section from the Non-Mixing CF/ABS to ABS sample set.

Considering the increased maximums, the change in transition direction could be considered to increase both the variation and hardness of the printed transition. However, Figure 9 shows a comparison of all three sample sets as a function of fiber content. This representation further indicates that an increased variation precedes any relevant increase in hardness when increasing fiber content, suggesting that there may be a critical level of fiber content in the sample before deformation resistance increases as a whole.

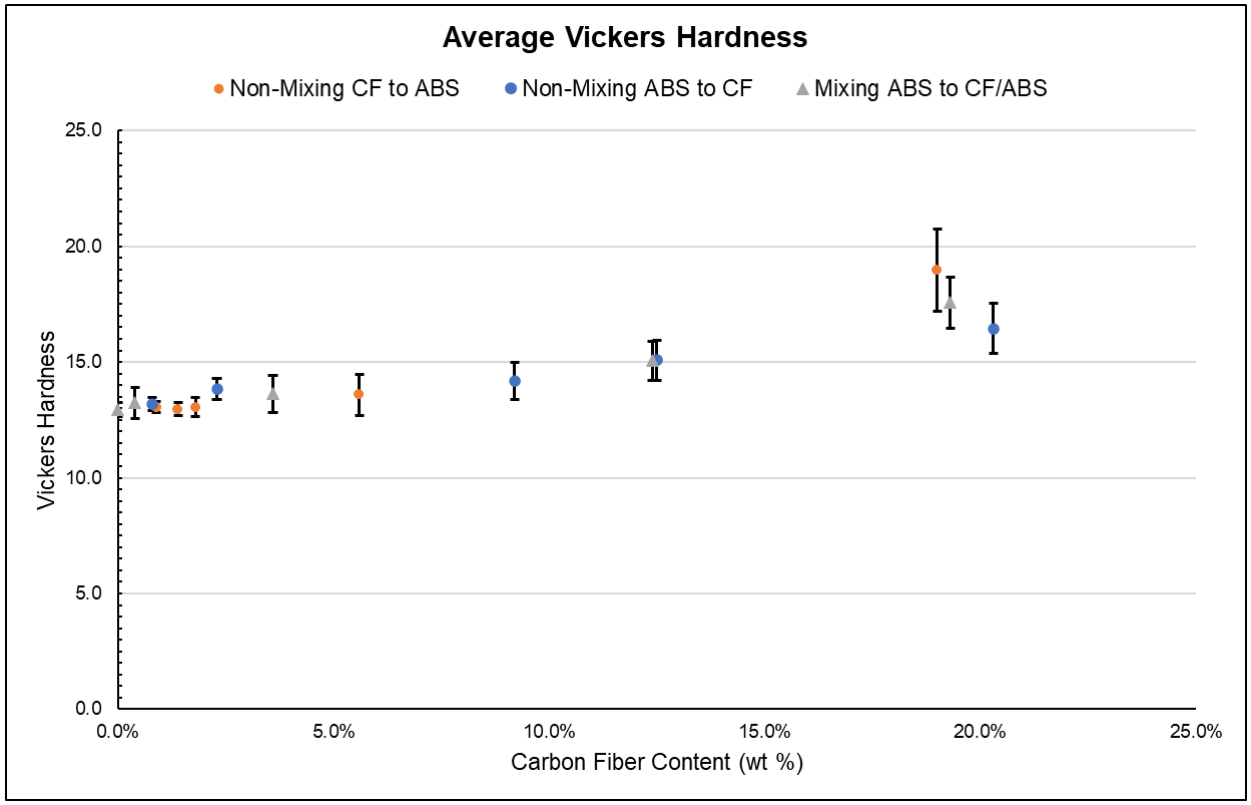

Figure 9: The average Vickers hardness value and standard deviation for all studied cross-sections as a function of fiber content.

Conclusions

Vickers Hardness of samples printed using the BAAM dual-hopper system is a useful characterization method for assessing the changes in mechanical performance surrounding the material transition region. The microhardness showed consistently different values based on the region of testing, i.e. carbon-fiber rich regions demonstrated a higher HV and greater resistance to deformation. The average HV of a cross-section increased with increasing fiber content by 24 % to 45 % depending on sample set. Similarly, the standard variation of the average hardness increased by 270 % to 620 %. This behavior indicated that fiber-rich regions both increased deformation resistance and contributed to an increased variation throughout the specimen. Furthermore, this behavior was constant regardless of experimental conditions. The change from a Non-Mixing to Mixing screw geometry provided no reduction in variation, though there was a 7 % increase in maximum HV. There was also little difference created by switching transition directions. While the Non-Mixing CF/ABS to ABS group did display a improved HV and greater standard deviation by 15 % and 61 %, respectively, compared to the Non-Mixing ABS to CF/ABS, the overall trends remained the same.

Future work will primarily focus on expanding the results of this study. A more comprehensive testing procedure will be used to investigate if increased sampling differentiates the Mixing and Non-Mixing geometries. The increased sampling will also be used to better analyze any positional trends in hardness within a single cross-section. Furthermore, a static mixing nozzle intended to improve blending of materials will also be utilized to print additional test specimens. Finally, a macroscopic characterization approach using Dynamic Mechanical analysis will also be included.

Acknowledgements

Research sponsored by the U.S. Department of Energy, Office of Energy Efficiency and Renewable Energy, Industrial Technologies Program, under contract DE-AC05-00OR22725 with UT-Battelle, LLC.

Thanks to Cincinnati Incorporated and Techmer PM for provided Material and Equipment.

Further thanks to the University of Tennessee – Knoxville Joint Institute for Advanced Materials, the Metallography Lab group at the Joint Institute for Advanced Materials, the National Science Foundation for additional funding, and the University of Tennessee – Knoxville Center for Materials Processing for collaboration and additional funding.

References

[1] C.E. Duty, V. Kunc, B. Compton, B. Post, D. Erdman, R. Smith, R. Lind, P. Lloyd, L. Love, Structure and mechanical behavior of Big Area Additive Manufacturing (BAAM) materials, Rapid Prototyping J 23(1) (2017) 181-189.

[2] T. Smith, A.A. Hassen, R. Lind, J. Lindahl, P. Chesser, A. Roschli, V. Kumar, V. Kishore, B. Post, J. Failla, C. Duty, L. Love, V. Kunc, Dual Material System for Polymer Large Scale Additive Manufacturing, Society for the Advancement of Material and Process Engineering 2020, Seattle, WA, 2020.

[3] J. Brackett, Y. Yan, D. Cauthen, V. Kishore, J. Lindahl, T. Smith, Z. Sudbury, H. Ning, V. Kunc, C. Duty, Characterizing material transitions in large-scale Additive Manufacturing, Additive Manufacturing 38 (2021) 101750.
[4] F. Wang, F. Ju, K. Rowe, N. Hofmann, Real-time control for large scale additive manufacturing using thermal images, 2019 IEEE 15th International Conference on Automation Science and Engineering (CASE), 2019, pp. 36-41.
[5] LSAM - Large Scale Additive Manufacturing, 2018. http://www.thermwood.com/lsam_home.htm#whatislsam. (Accessed September 9 2021).
[6] A. Wedgewood, P. Pibulchinda, E.B. Vaca, C. Hill, M.J. Bogdanor, Materials Development and Advanced Process Simulation for Additive Manufacturing with Fiber-Reinforced Thermoplastics, ; IACMI The Composite Institute, 2021, p. Medium: ED.
[7] D. Moreno Nieto, V. Casal López, S.I. Molina, Large-format polymeric pellet-based additive manufacturing for the naval industry, Additive Manufacturing 23 (2018) 79-85.
[8] ASTM, Standard Test Method for Rubber Property - Durometer, 2021.
[9] W.D. Vian, N.L. Denton, Hardness Comparison of Polymer Specimens Produced with Different Processes, American Society for Engineering Education Illinois-Indiana Section, 2018.
[10] S. Zheng, I. Ashcroft, A depth sensing indentation study of the hardness and modulus of adhesives, International Journal of Adhesion and Adhesives - INT J ADHES ADHES 25 (2005) 67-76.
[11] A. Turnbull, D. White, Nanoindentation and microindentation of weathered unplasticised poly-vinyl chloride (UPVC), J Mater Sci 31(16) (1996) 4189-4198.
[12] J. Payandehpeyman, G. Majzoobi, R. Bagheri, Experimental and analytical investigations into the effects of inorganic filler on the polypropylene nanocomposite microhardness, Journal of Thermoplastic Composite Materials 30(11) (2017) 1484-1502.
[13] T. Melo-Silva, C. de Melo-Silva, C. Carvalho, A. Teixeira, E.C. Carvalho, A.S. Carvalho, F.A. Araujo, A.M. Nunes, J. Lins, J. Gouvêa, Evaluation of Load Parameters and Hold Time of a Vickers Ultra-Micro Hardness Tester for Measure of Hardness and Modulus of Elasticity of Dental Composites, Materials Science Forum 912 (2018) 130-135.
[14] J. Brackett, D. Cauthen, T. Smith, V. Kunc, C. Duty, The Influence of Processing Parameters on the Transition Zone for Blended Material 3D Printing, Society for the Advancement of Material and Process Engineering 2020, Seattle, WA, 2020.
[15] J. Brackett, E. Charles, D. Cauthen, T. Smith, V. Kishore, V. Kunc, E. Duty Chad, The Impact of Processing Parameters on the Transition Behavior of Blended Material Large Scale 3D Printing, In Preparation (2021).
[16] A. International, ASTM E384-17, Standard Test Method for Microindentation Hardness of Materials, West Conshohocken, PA, 2017.